Project no. 505428 (GOCE)

AquaTerra

Integrated Modelling of the river-sediment-soil-groundwater system; advanced tools for the management of catchment areas and river basins in the context of global change

Integrated Project

Thematic Priority: Sustainable development, global change and ecosystems

Deliverable No.: BASIN R3.30 (Meuse)
Title: Report on the development of the Geer Hydrological model. Final results about climate change impacts evaluation.

Due date of deliverable: March 2009
Actual submission date: March 2009

Start date of project: 01 June 2004   **Duration: 60 months**

Organisation name *and contact* of lead contractor *and other contributing partners* for this deliverable:

P. Goderniaux, S. Brouyère, Ph. Orban, A. Dassargues
Group of Hydrogeology and Environmental Geology - Aquapôle ULg
University of Liège, Building B52/3, 4000 Sart Tilman, Belgium
Tel: +32.43.662377/ Fax: +32.43.669520, Serge.Brouyere@ulg.ac.be

H.J. Fowler, S. Blenkinsop
Water Resource Systems Research Laboratory - School of Civil Engineering and Geosciences
Cassie Building - Newcastle University
Newcastle upon Tyne NE1 7RU United Kingdom

Revision: M. Finkel

Project co-funded by the European Commission within the Sixth Framework Programme (2002-2006)		
Dissemination Level		
PU	Public	
PP	Restricted to other programme participants (including the Commission Services)	
RE	Restricted to a group specified by the consortium (including the Commission Services)	
CO	Confidential, only for members of the consortium (including the Commission Services)	**X**

SUMMARY

In the framework of Workpackage BASIN R3 Meuse, the Hydrology Group of the University of Liège (Belgium) has developed a hydrological model of the Geer sub-catchment, in order to assess climate change impacts on groundwater reserves. The water resource Systems Research Laboratory of the Newcastle University has produced the climate change scenarios applied on the hydrological model.

This report describes the methodology used, the implementation of the hydrological model, the climate change scenarios and the results of the study.

This deliverable is in the form of a manuscript that has been submitted to 'Journal of Hydrology'.

17/10/2008 : submission to 'Journal of Hydrology'

24/01/2009 : accepted with moderate revisions

05/03/2009 : re-submission of the revised manuscript

MILESTONES REACHED (from DOW 5)

No milestones are associated to this deliverable

Using the meteorological data available for the Geer basin, HYDRO 1 has generated climate change scenarios applied as input to the hydrological model.

Table of contents

List of tables

List of figures

Large scale surface – subsurface hydrological model to assess climate change impacts on groundwater reserves

Pascal GODERNIAUX[1,2,*], Serge BROUYERE[1], Hayley J. FOWLER[3], Stephen BLENKINSOP[3], René THERRIEN[4], Philippe ORBAN[1], Alain DASSARGUES[1]

[1]Group of Hydrogeology and Environmental Geology – Aquapôle
University of Liège
Chemin des Chevreuils, 1
Building B52/3
4000 Liège
Belgium

[2]National Funds for Scientific Research of Belgium
Rue d'Egmont, 5
1000 Brussels
Belgium

[3]Water Resource Systems Research Laboratory
School of Civil Engineering and Geosciences
Cassie Building
Newcastle University
Newcastle upon Tyne NE1 7RU
United Kingdom

[4]Department of Geology and Geological Engineering
Université Laval
G1K 7P4 Quebec (Quebec)
Canada

Abstract

Estimating the impacts of climate change on groundwater represents one of the most difficult challenges faced by water resources specialists. One difficulty is that simplifying the representation of the hydrological system often leads to discrepancies in projections. This study provides an improved methodology for the estimation of the impacts of climate change on groundwater reserves, where a physically-based surface – subsurface flow model is combined with advanced climate change scenarios for the Geer basin (465 km²), Belgium. Coupled surface–subsurface flow is simulated with the finite element model HydroGeoSphere. The simultaneous solution of surface and subsurface flow equations in HydroGeoSphere, as well as the internal calculation of the actual evapotranspiration as a function of the soil moisture at each node of the defined evaporative zone, improve the representation of interdependent processes like recharge, which is crucial in the context of climate change. More simple models or externally coupled models do not provide the same level of realism. Fully integrated surface – subsurface flow models have recently gained attention, but have not been used in the context of climate change impact studies. Climate change simulations were obtained from 6 regional climate model (RCM) scenarios assuming the SRES A2 emission (medium-high) scenario. These RCM scenarios were downscaled using a quantile mapping bias-correction technique that, rather than applying a correction only to the mean, forces the probability distributions of the control simulations of daily temperature and precipitation to match the observed distributions. The same corrections are then applied to RCM scenarios for the future. Climate change scenarios predict hotter and drier summer and warmer and wetter winters. The combined use of an integrated surface – subsurface modelling approach, a spatial representation of the evapotranspiration processes and sophisticated climate change scenarios improves the model realism and projections of climate change impacts on groundwater reserves. For the climatic scenarios considered, the

integrated flow simulations show that significant decreases are expected in the groundwater levels (up to 8 meters) and in the surface water flow rates (between 9% and 33%) by 2080.

1. Introduction and objectives

Estimating the possible impacts of climate change on water resources represents one of the most difficult challenges faced by water managers. Because of the great interest in such projections, several studies have been recently published on the topic (see for example Christensen et al., 2004; Fowler et al., 2003; Fowler et al., 2007b; VanRheenen et al., 2004). Most of these studies focus on surface water and generally oversimplify or even neglect groundwater, although groundwater is the main water supply in many parts of the world. Additionally, studies that try to assess climate change impact on water resources are likely to produce variable results (Jiang et al., 2007). One of the main reasons for the discrepancy in projections is that simplistic assumptions are often made to represent the physical processes associated with hydrological systems. This is particularly the case for the studies that account for groundwater, where the representation of processes associated with subsurface flows and groundwater recharge brings additional complexity. These assumptions increase the uncertainty associated with model projections and need to be addressed.

A first requirement for estimating the impact of climate change on groundwater systems is a reliable estimate of the volume of water entering and leaving an aquifer. More specifically, a reliable estimate of groundwater recharge is needed because it represents the connection between atmospheric and surface-subsurface processes and is therefore a key element in the context of the impacts of climate change on groundwater. Similarly, in aquifers strongly influenced by surface water, groundwater discharge into rivers may be affected by changes in surface water levels, and consequently affect groundwater levels (Scibek et al., 2007). In previous studies (see for example Brouyère et al., 2004a; Chen et al., 2002; Holman, 2006; Loáciga, 2003; Scibek et al., 2007; Serrat-Capdevila et al., 2007; Woldeamlak et al., 2007), recharge has been estimated with various degrees of complexity, ranging from simple linear functions of precipitation and temperature (Chen et al., 2002; Serrat-Capdevila et al.,

2007) to the application of "soil models" simulating variably-saturated groundwater flow and solute transport (Allen et al., 2004; Brouyère et al., 2004a; Scibek and Allen, 2006). However, none of these previous models can simulate the feedback, or fluid exchange, between the surface and subsurface domains. This feedback is an integral component of the water cycle since groundwater recharge depends on precipitation and evapotranspiration at the surface domain, evapotranspiration in the vadose zone, evapotranspiration in the saturated zone when water levels are close to the ground surface, and finally river – aquifer interactions. The quantitative estimation of the latter four fluxes depends on the simulation of simultaneous hydraulic conditions in the surface and subsurface domains. Therefore, estimating recharge by only considering one part of the whole system is unrealistic, inaccurate and potentially unusable in the context of climate change impact assessments. Similarly, loosely coupled modelling approaches, where water exchange between surface and subsurface is calculated independently, do not provide a sufficient level of realism because they do not solve for all the interdependent processes simultaneously.

A second requirement for estimating the impact of climate change on groundwater systems is that hydrogeological system models must be capable of consistently representing observed phenomena, which is not always the case. For example, Chen et al. (2002) estimated the impact of climate change on a Canadian aquifer with an empirical model that links piezometric variations and groundwater recharge, where recharge is assumed to be a linear function of precipitation and temperature. Most studies focussing on surface water, such as Arnell (2003), also use simplistic transfer functions to represent exchanges between ground- and surface water. However, such transfer functions often oversimplify the exchange processes. These functions can still be substituted for more detailed physical representations for specific conditions if they are verified with calibration, but their use may become uncertain if applied stresses go beyond the calibration conditions, which is typical for climate

5

change scenarios. Detailed physically-based and spatially-distributed models that take into account hydrogeologic processes provide more realistic simulations of groundwater fluxes, including exchanges with surface water.

In addition to the choice of modelling approach, the need for high resolution climate scenarios adds an additional layer of complexity and uncertainty to future projections. Large-scale General Circulation Models (GCMs) contain uncertainties both in the structures used to represent large-scale climate processes and by the incorporation of the effects of small-scale physics through the parameterization of unresolved processes. Any single model simulation of future climate therefore represents only one of many possible future climate states. Furthermore, due to the mismatch of scales between climate model output and that of hydrological models, some form of "downscaling" is required to produce output at an appropriate scale to model impacts on hydrological systems (for a review of downscaling methods, see Fowler et al., 2007a; Wilby and Wigley, 1997). The dynamical downscaling approach uses physically-based regional climate models (RCMs) driven by conditions provided by a GCM to produce finer-scale output (typically about 0.5°). However, further statistical downscaling is generally required for hydrological modelling. To date, studies examining the impacts of changes in climate on groundwater systems have adopted relatively simple statistical downscaling methods and have tended to use a small ensemble of climate models. One of the most straightforward approaches is the 'perturbation' or 'delta change' method (Prudhomme et al., 2002) which applies 'change factors' (CFs), calculated as difference between the control and future GCM simulations, to observations (e.g. Brouyère et al., 2004a; Yusoff et al., 2002). However, since these scenarios were produced by applying the projected changes to mean temperature and precipitation to the whole of the corresponding future distribution, they fail to reflect changes in the shape of the distribution, which is important for extremes or changes in the distribution of wet and dry periods.

The objective of this study is to provide improved methods for the estimation of the impacts of climate change on groundwater reserves, by developing a modelling approach that alleviates the simplifying assumptions presented above. The approach also includes an improved climate downscaling method that applies a correction across the distributions of temperature and precipitation using output from state-of-the-art RCM simulations.

To demonstrate the approach, a numerical model has been used to develop catchment-scale simulation of coupled surface and subsurface water flow in the Geer basin located in the Walloon Region of Belgium. The physically-based and spatially-distributed numerical model used here provides a realistic representation of the system, compared to simplified models that are inadequate if the water fluxes extrapolated in the climate change scenarios and imposed to the hydrologic system are not included in the intervals of values used in the calibration procedure. The model developed in this study fully integrates surface- and subsurface- flow in the saturated and partially saturated zones, with a simultaneous solution of the flow equations in all domains using finite elements. This simultaneous solution enables a better representation of the whole system because water flow in one domain is interconnected with flow in the other domains. Water exchange between the surface and subsurface nodes is calculated internally at each time step. Similarly, the actual evapotranspiration is calculated internally as a function of the soil moisture at each node of the defined evaporative zone and at each time step. Integrating evapotranspiration, surface, and subsurface flow calculations in the same model does not only increase the complexity of the model, which would not guarantee more robust predictions (Ebel and Loague, 2006), but also increases the number of observed data available for calibration. Because both surface and subsurface data are used for calibration, parameter values are better constrained, and the uncertainty in the estimation of some components of the global water balance is reduced, in particular recharge and surface water – groundwater interactions. The development and use of such fully integrated surface –

subsurface models has recently gained attention. Fully integrated simulations typically require substantial computer resources and most simulations published have been either limited to small catchments or short time periods. For example, Jones (2005) and Sudicky et al. (2008) developed a model for a 75 km² catchment (Laurel Creek Watershed – Ontario, Canada). The finite element grid representing the catchment contained more than 600,000 nodes and transient simulations of coupled surface and subsurface flow over a period of 1 month, with specified fluxes input on a hourly basis, took more than 4 days of computational time (3.2 GHz Pentium4 desktop machine equipped with 4.0 Gb RAM). Another example is reported by Li et al. (2008), who modelled surface and subsurface flow, and evapotranspiration fluxes for a 286 km² catchment (Duffins Creek Watershed – Ontario, Canada) with more than 700,000 nodes and made transient simulations over 1 year periods with specified fluxes input on a daily basis. To our knowledge, there are very few examples of such integrated surface – subsurface models used in the context of climate change impact evaluation (e.g. Van Roosmalen et al., 2007). The integrated model of the Geer basin has been developed for a catchment area of 465 km² and transient simulations are run from 2010 to 2100, which is a challenging test of the modelling methodology compared to the short time-scale transient simulations more usually performed with fully integrated surface – subsurface flow models.

The combined use of an integrated surface – subsurface modelling approach, a spatial representation of the evapotranspiration processes and advanced climate change scenarios should greatly improve the robustness of projections of the impacts of climate change on groundwater.

Section 2 of this paper describes the geological and hydrological contexts of the Geer basin. Section 3 presents the conceptual assumptions made to implement the model, the finite element code, the discretisation of the catchment, the variables and parameters, and the results

8

of the calibration procedure. Section 4 describes the climate change scenarios used in this study and the results of their application in the implemented hydrological model. Last sections provide a discussion of the results and conclude the study.

2. The Geer basin

The Geer sub-catchment is located in eastern Belgium, north-west of the city of Liège, in the intensively cultivated 'Hesbaye' region. The hydrological basin extends over approximately 480 km², on the left bank of the Meuse River (Figure 1).

The geology of the Geer basin essentially consists of Cretaceous chalky formations that dip northward and that are bounded at their base by 10 metres of smectite clays of very low hydraulic conductivity (Figure 2). The chalk formation consists of a series of chalk layers, whose thicknesses range from a few meters up to 70 m. A flint conglomerate of dissolved chalk residues overlies the chalk, with a maximum thickness of 10 m. Tertiary sand lenses of small extension are found locally above this conglomerate and a thick layer (up to 20 m) of Quaternary loess is observed throughout the catchment. Tertiary sands and clays entirely cover the chalk formations north of the Geer River (Figure 2) (Hallet, 1998; Orban et al., 2006).

The main aquifer in the region is the 'Hesbaye' aquifer, which corresponds to the chalk layers and is unconfined over most of the basin. Subsurface flow is from south to north and the aquifer is mainly drained by the Geer River that flows from west to east (Orban et al., 2006). The chalk porous matrix, whose total porosity is estimated equal to 44%, enables the storage of large quantities of groundwater, while fast preferential flow occurs through fractures, which represent approximately 1% of the total porosity (Brouyère, 2001; Hallet, 1998). At a macroscopic scale, the hydraulic properties of the chalk formations vary vertically and laterally. The lower Campanian chalks are usually less permeable than the upper

9

Maastrichtian chalks. Laterally, zones of higher hydraulic conductivity are observed and associated with 'dry valleys', mostly oriented south to north. These zones, characterized by a higher degree of fracturing, are associated with a slight lowering of hydraulic heads. For the larger part of the Geer catchment, the saturated zone is exclusively located in the chalk formations. The thick loess layer located above the chalk controls the water infiltration rate from the land surface to the chalky aquifer, resulting in smoothed recharge fluxes at the groundwater table and attenuation of seasonal fluctuations of hydraulic heads that are better characterised by multi-annual variations (Brouyère et al., 2004b). In the northern part of the catchment, near the Geer River, water levels are closer to the ground surface and semi-confined conditions may prevail because of the loess Quaternary deposits. North of the Geer River, Tertiary deposits become thicker and contain some clearly clayey layers. These layers are responsible for the confined nature of the chalky aquifer at this location (Figure 2).

The 'Hesbaye' aquifer is largely exploited for drinking water, primarily through a network of pumping galleries of more than 40 km that is located in the saturated chalk formation (Figure 1). According to Hallet (1998), extracted groundwater volumes represent between 6% and 11% of annual precipitation. The groundwater budget (Hallet, 1998) indicates groundwater losses mostly through the northern catchment boundary, and partly resulting from groundwater extraction in the Flemish region of Belgium located directly north of the Geer basin. The Hesbaye aquifer suffers from severe nitrate contamination problems, due to intensive agricultural activities. In many locations in the unconfined part of the aquifer, nitrate concentrations are frequently over 45 mg/L, approaching the drinking water limit of 50 mg/L (Batlle-Aguilar et al., 2007; Hallet, 1998).

3. Modelling

3.1 Conceptual model

The Geer hydrological catchment defines the boundaries of the modelled area (Figure 1). The smectite clay (Figure 2) is considered impervious and the contact between the clay and the chalk represents the lower boundary of the model. The western, southern and eastern boundaries correspond to surface water divides and it is assumed that there is no water exchange across these boundaries for either surface or subsurface flow. On the other hand, groundwater fluxes through the northern boundary must be taken into account. Along this border, hydrogeological and hydrographical limits differ, and groundwater flows northwards towards the adjacent basin.

The Geer River at the level of the 'Kanne' gauging station, located 4 kilometres upstream from the confluence with the Meuse River, is considered as the outlet of the catchment. Surface water exchanges are not observed elsewhere along the model boundaries, since they correspond to topographical limits.

Pumping wells operated by water supply companies or farmers are distributed over the whole basin but water collected through the network of draining galleries is the largest component of the total of groundwater abstraction in the Geer basin.

3.2 Mathematical and numerical model

The Geer basin hydrological model has been developed with the HydroGeoSphere finite element model (Therrien et al., 2005). The spatially-distributed model simulates fully coupled 3D variably saturated groundwater flow in granular or fractured aquifers and 2D overland flow, as well as solute transport in the surface and subsurface domains. HydroGeoSphere simulates the dynamic interactions between all sub-domains at each time step. It partitions rainfall into components such as evapotranspiration, runoff and infiltration.

11

The model also allows the calculation of water infiltration or exfiltration between rivers and aquifers. These interactions are of great interest in the context of climate change as recharge is very sensitive to climatic variations and represent crucial elements for impacts projections.

HydroGeoSphere uses the control volume finite element approach to simultaneously solve Richards' equation describing 3D variably-saturated subsurface flow and a 2D depth-averaged surface flow equation, which is the diffusion-wave approximation of the Saint Venant equation. In the subsurface domain, the hydraulic head, the degree of saturation, and the water Darcy flux are calculated at each node in the grid. In the surface domain, water depth ($\approx$ height of water above ground surface) and fluid flux are calculated for each node of the 2D grid. The stream locations can be implicitly retrieved by considering the surface nodes where the water depth is greater than zero. Transport processes include advection, dispersion, retardation and decay. Newton-Raphson iterations are used for solving non-linear equations. More information on the model and equations solved is available in Therrien et al. (2005) and in Li et al (2008).

Hydrologic parameters required for the fully-coupled simulation are listed in Table 1 along with their domain of application. It should be noted that fractures are not represented explicitly in the Geer basin model, and equivalent porous media properties are assigned to the elements representing the aquifer.

The Geer basin model uses a 'dual-node approach' to calculate water exchanges between the surface and subsurface domains. In this approach, surface nodes have to coincide with nodes of the subsurface grid topmost layer. Water flux between each corresponding surface and subsurface nodes is calculated as the hydraulic head difference between the two domains multiplied by a leakage factor (coupling length – L_e [L]) characterising the properties of the soil. In HydroGeoSphere, the model of Kristensen and Jensen (1975) is used to

calculate the actual transpiration T_p [LT^{-1}] and evaporation E_s [LT^{-1}] as a function of the potential evapotranspiration E_p [LT^{-1}], the soil moisture at each node belonging to the specified evaporative and root zones, and the 'Leaf Area Index' (LAI [-]) that represents the cover of leaves over a unit area (Equation 1 to 6) (Therrien et al., 2005). Equation 2 expresses the vegetation term, as a function of LAI, and parameters C_1 and C_2. Full transpiration can occur if water saturation θ [-] is higher than θ_{t1} and there is no transpiration if water saturation is lower than θ_{t2}. Between these two limiting saturations, transpiration decreases following a law governed by the parameters C_3 (Equations 1 and 3). RDF(L_r) is the 'Root Distribution Function' that distributes the water extracted from the root zone, along the root depth L_r [L], following a quadratic law. The quantity of extracted water is more important near the surface and decreases with depth until zero at the root depth L_r. The 'canopy evaporation E_{can} [LT^{-1}] corresponds to the evaporation of water intercepted by the canopy. Full evaporation can occur if water saturation is higher than θ_{e1} and there is no evaporation if water saturation is lower than θ_{e2}. Between these two limits, evaporation decreases following a law governed by parameter C_3 (Equations 4 and 5). EDF(L_e) is the 'Evaporation Distribution Function' that distributes the water extracted from the evaporative zone, along the evaporation depth (L_e), following a quadratic law. The interception of precipitation by the canopy is simulated by the bucket model, where precipitation in excess of interception storage and evapotranspiration reaches the ground surface. The 'interception storage capacity' S_{int}^{max} [L] represents the maximum quantity of water that can be intercepted by the canopy. It depends on LAI and the 'canopy storage parameter' c_{int} [L] (Equation 6).

$$T_p = f_1(LAI) \times f_2(\theta) \times RDF(L_r) \times \left[E_p - E_{can} \right] \tag{1}$$

$$f_1(LAI) = \max\left\{ 0, \min\left[1, \left(C_2 + C_1 \times LAI \right) \right] \right\} \tag{2}$$

$$f_2 = \begin{cases} 0 & for & 0 \le \theta \le \theta_{t2} \\ 1 - \left[\dfrac{\theta_{t1} - \theta}{\theta_{t1} - \theta_{t2}} \right]^{C_3} & for & \theta_{t2} \le \theta \le \theta_{t1} \\ 1 & for & \theta_{t1} \le \theta \end{cases} \qquad (3)$$

$$E_s = \alpha^* \times \left(E_p - E_{can} \right) \times \left[1 - f_1(LAI) \right] \times EDF(L_e) \qquad (4)$$

$$\alpha^* = \begin{cases} 0 & for & \theta < \theta_{e2} \\ \dfrac{\theta - \theta_{e2}}{\theta_{e1} - \theta_{e2}} & for & \theta_{e2} \le \theta \le \theta_{e1} \\ 1 & for & \theta > \theta_{e1} \end{cases} \qquad (5)$$

$$S_{int}^{max} = c_{int} \times LAI \qquad (6)$$

3.3 Discretisation

A three-dimensional finite element mesh, composed of several layers of 6-node triangular prismatic elements (Figure 3), was generated based on the conceptual model presented previously. The elements have lateral dimensions equal to approximately 500 m. The top and bottom layers of nodes represent the soil surface and the contact between smectite clay and chalk, respectively. Subsurface formations are discretised using 11 finite element layers. Five layers are used for the first five meters below the ground surface, with each layer having a thickness of one meter. The finer vertical discretisation near ground surface represents more accurately river – aquifer interactions as well as recharge processes at the interface between the surface and subsurface domains. In particular, distributing several nodes vertically within the first few meters below the ground surface enables the variation of evaporative and root depths, as well as the vertical distribution of evapotranspiration rates, according to the land use and soil type. The remaining lower six finite element layers are uniformly distributed vertically between the fifth and bottom layers. A material is assigned to each 3D finite element based on data from more than 120 boreholes distributed throughout the

catchment. The ground surface is discretised using one layer of 2D finite elements (Figure 3). The elevation of the surface nodes are calculated using the Geer basin DTM (Digital Terrain Model), whose pixels have dimensions equal to 30×30 m. In the dual node approach, the nodes forming the surface domain correspond to the node of the top layer of the subsurface domain. The total number of nodes for the subsurface and surface domains is equal to 9420 and 785, respectively.

No-flow boundaries are applied to subsurface nodes belonging to the western, southern, eastern and bottom boundaries. Cauchy conditions (head dependent flux) are applied on the subsurface nodes along the northern boundary to take into account groundwater losses in the direction of the adjacent catchment located northward from the Geer basin. For the surface flow domain, no-flow Neumann boundary conditions are prescribed along the hydrographical limits of the Geer basin. Critical-depth boundary conditions are prescribed at the nodes corresponding to the catchment outlet, at the level of the 'Kanne' gauging station. A critical-depth boundary condition forces the water elevation at the boundary to be equal to the 'critical depth'. The 'critical depth' is the water elevation for which the energy of the flowing water relatively to the stream bottom is minimum (Hornberger et al., 1998; Therrien et al., 2005).

3.4 Specified Fluxes

Specified hydrological fluxes within the Geer catchment consist of precipitation, evapotranspiration and groundwater abstraction by draining galleries and pumping wells.

Historical climatic data are available for several weather stations located inside or near the Geer basin[1] (more details in Orban et al., 2006). The stations shown in Figure 1 have complete precipitation (P) time series from 1960 to 2005. Temperature (T) and potential evapotranspiration (PET) data, for the same time period, are available for the Bierset station only. Data from these weather stations are used as inputs to the model and are applied on the surface node layer as transient specified fluxes. Precipitation data from each station are distributed using Thiessen polygons. Potential evapotranspiration data available only for the Bierset station are assumed to be applicable to the whole catchment.

Extracted groundwater volumes, from the draining galleries and from the most important production wells (Figure 1), have been collected by the Walloon administration and are updated annually (Orban et al., 2006). Transient volumetric flow rates are prescribed at each node of the 3D grid corresponding to the draining galleries or the pumping wells locations.

3.5 Calibration procedure

The model was calibrated to observed hydraulic heads and surface flow rates during the period 1967-2003. A preliminary calibration was performed in steady state conditions, using the mean data of the hydrologic year 1967-1968, and the results were used as initial conditions for the transient simulations. Calibration further showed that inaccuracies in these initial conditions only affect the simulation results on a short-term basis. Even with initial conditions very different from reality, such as a fully saturated subsurface domain, induced differences are reduced within a few days for surface water flow rates and within 2 years for groundwater hydraulic heads. The transient flow model is calibrated to surface flow rates

---

[1] Historical climatic data for the Geer catchment were obtained from the Royal Meteorological Institute of Belgium (RMI).

measured at the 'Kanne' gauging station located on the Geer river at the catchment outlet, and to hydraulic heads from 9 observation wells selected according to their location and the availability of measured hydraulic heads during the calibration period (Figure 1). In order to limit computational time, specified fluxes are input on a monthly basis, using mean monthly precipitation, evapotranspiration and groundwater abstraction rates. Adaptive time-stepping is used so that groundwater hydraulic heads and surface water elevations do not vary by more than 0.5 m and 0.01 m, respectively, during one time step. For the Geer basin model, time steps commonly vary between 1 hour and 1 day.

In the subsurface domain, the van Genuchten parameters are prescribed according to Brouyère (2001) and Brouyère et al. (2004b). Table 2 summarizes the values used for the chalk and loess formations. Saturated hydraulic conductivities are adjusted during calibration, taking into account the extension of the geological units and the zones of higher hydraulic conductivity associated with 'dry valleys'. The chalky aquifer is also vertically divided into 3 zones, namely 'upper chalk', 'intermediate chalk' and 'lower chalk'. This enables the representation of the decrease of saturated hydraulic conductivity with depth. Adjusted values are also kept within ranges provided by the measurements from laboratory and field tests conducted in the geologic formations of the Geer basin, and by ranges of hydraulic conductivity values given by Hallet (1998), Brouyère (2001), Brouyère et al. (2004b), and Dassargues and Monjoie (1993) for the Geer basin formations. Table 3 and Figure 4 summarize all saturated hydraulic conductivity values at the end of the calibration.

In the surface domain, the coupling length and the friction coefficients were adjusted according to the soil[2] and land use[3] maps, respectively. The soil mean characteristics and

---

[2] © Direction Générale de l'Agriculture (Ministère de la Région Wallonne). Projet de Cartographie Numérique des sols de Wallonie (PCNSW). Projet du Gouvernement Wallon (GW VIII/2007/Doc.58.12/12.07/B.L & GW VII/2000/Doc.1331/07.12/JH.)

thicknesses are quite homogeneous at the scale of a 2D surface element in this model, since these characteristics vary at a much smaller scale. The coupling length was therefore assumed constant everywhere and equal to 0.01 m. Calibration later showed that the results were insensitive to the value of the coupling length. Three categories of land-use, namely 'rural', 'urban' and 'forested', have been identified and Manning's roughness coefficients were initially defined for each category. The values of Manning's roughness coefficients obtained at the end of the calibration (Table 4) are abnormally high compared to values more commonly used in hydrological models (Hornberger et al., 1998; Jones, 2005; Li et al., 2008). These high values are the result of the coarse time and space discretisations used to represent the Geer basin. Additional simulations, not presented here, that used specified fluxes input on a daily basis during a shorter total simulation time showed that the results of the calibration were highly dependent upon the time discretisation of precipitation and evapotranspiration, especially for parameters linked to the surface domain. These additional simulations also showed that, when specified fluxes are input on a daily basis for the Geer basin model, calibrated friction coefficient values were smaller and comparable to more commonly used values.

The parameters used to calculate the actual evapotranspiration (Kristensen and Jensen, 1975) were defined using values found in the literature and are summarised in Table 5 for four land-use categories (rural crop, rural grassland, rural broadleaf deciduous forested, urban). Root depths range between 0 m and 5.2 m, according to values given by Canadell et al. (1996). A uniform evaporation depth value of 2 m is assumed over the whole catchment. Values for the maximum Leaf Area Index (LAI) are given by Scurlock et al. (2001), Asner et al. (2003), Vasquez and Feyen (2003) and Li et al. (2008). Breuer et al. (2003) give maximum

---

[3] European Environment Agency (http://www.eea.europa.eu). Corine Land Cover Project. Copyright

and minimum values of the LAI throughout the year. For the Geer basin model, maximum LAI varies from 0.40 to 5.12. In absence of information about minimum LAI for the vegetation of the Geer basin, LAI is arbitrarily reduced by 50 % during the winter months. However, the results are insensitive to the value of Min. LAI given that evapotranspiration is very low during winter months anyway. Values for the empirical transpiration fitting parameters C1, C2 and C3, as well as for the canopy storage interception C_{int} can be found in Kristensen and Jensen (1975) and Li et al. (2008). Used values of C1, C2, C3 and C_{int} are equal to 0.3, 0.2, 10 and 1×10^{-5} m, respectively. The limiting saturations, corresponding to the wilting point and field capacity, are specified as the saturations corresponding to pF values[4] equal to 4.2 and 2.5, as found in Brouyère (2001).

Results of the steady state and transient simulations, using the calibrated parameters, are shown in Figure 5, Figure 6 and Figure 7. Figure 5A presents the computed steady-state subsurface saturations for the hydrological year 1967-1968. Similarly, Figure 5B**Fehler! Verweisquelle konnte nicht gefunden werden.** shows the computed steady-state water elevation at each node of the surface domain. The locations of the Yerne and the Geer Rivers are clearly seen and correspond to the highest water elevations. Figure 6 presents the measured and simulated transient hydraulic heads for the 9 selected observation wells. Table 6 shows the mean absolute error and the mean error values between observed and computed heads. Generally, computed heads are higher than observed heads, except in A7-PL37. The mean absolute error varies from 1.7 m for XHE015 to 8.4 m for SLI006. The higher errors for SLI006 and A7-PL37 could be explained by the proximity of the model borders, where the boundary conditions may not be verified locally. In particular, groundwater losses through the northern catchment boundary may be variable along this border, while they are simulated in

EEA, Copenhagen, 2007.

19

the model using a uniform 'head dependent flux' boundary condition. Additionally, observations are quite limited at SLI006, which makes the evaluation of the calibration less reliable. Seasonal variations, as calculated by the model, are slightly too high at some observation wells, especially for 'VIE044', where the groundwater level is close to the ground surface. However, simulated heads satisfactorily reproduce the multi-annual variations in groundwater levels. Figure 7 presents the measured and simulated transient flow rates for the 'Kanne' gauging station located at the outlet of the basin. The simulated flow rates are of the same order of magnitude as the observed flow rates. Computed values match well to observed values in summer, for low flow rates and recession periods. Differences remain for the winter, where simulated flow rates are too high compared with observed flow rates. The water balance analysis shows that the model overestimates by 6% of the total precipitation the water flow rates at the 'Kanne' gauging station. Table 7 shows the main components of the water budget for the simulation performed between 1967 and 2003.

4. Simulation of climate change scenarios

As stated previously, the integrated Geer basin model has been specially developed to assess the possible impacts of climate change on groundwater resources. As a next step climate change scenarios are therefore applied to the basin model and projected changes and uncertainties are assessed.

4.1 Climate scenarios

In order to assess the likely impacts of climate change on water resources for the Geer catchment, Regional Climate Model (RCM) output from the European Union Fifth Framework Programme (FP5) PRUDENCE project (Prediction of Regional scenarios and

---

[4] pF=log(-hydraulic pressure)

Uncertainties for Defining EuropeaN Climate change risks and Effects) (Christensen et al., 2007) was used. These dynamic climate models provide a series of high-resolution simulations of European climate for a control simulation (1961-1990) and for a future time period (2071-2100). These are the results of a series of "time-slice" experiments, each representing a stationary climate over the selected 30-year period, whereby a climate model is allowed to fully adjust to an equilibrium state in response to a prescribed radiative forcing, i.e. the simulations reflect variability about an equilibrium state over a 30-year period. In addition to the uncertainty introduced by the choice of RCM, each model derives its boundary conditions from a different GCM, with each GCM representing atmospheric processes differently, either through different numerical schemes or different parameterisations. One way of addressing these uncertainties is through the use of multi-model ensembles. Here, we use an ensemble of 6 RCM simulations (Table 8) with boundary conditions derived from what may be considered as two different GCMs, the HadAM3H atmosphere only model (Gordon et al., 2000; Pope et al., 2000) and the ECHAM4/OPYC coupled atmosphere-ocean model (Roeckner et al., 1996). The HadRM3P and ARPEGE RCM simulations derive boundary conditions from HadAM3P and the coupled atmosphere-ocean model HadCM3 respectively. Both HadAM3H and HadAM3P are dynamically downscaled to an intermediate resolution from the HadCM3 coupled atmosphere-ocean model and are thus closely related. Further details on the RCMs used within PRUDENCE may be found in Jacob et al. (2007).

Here, only projections using the SRES A2 emissions (medium-high) scenario (Nakicenovic et al., 2000) are examined as recent observed increases in atmospheric carbon dioxide concentrations are in accordance with projections from high emissions scenarios (Rahmstorf et al., 2007). However, significant divergence in greenhouse gas concentrations between scenarios in the second half of the 21st century generates uncertainty in future climate forcing. Although this uncertainty arising from future emissions is not examined here

it is discussed within the context of the final results in Section 6. For each RCM, mean daily temperature and daily total precipitation were extracted for the control and future time periods for the RCM grid cells overlying the meteorological stations shown in Figure 1.

4.2 Downscaling of RCM output

Even the relatively high-resolution RCMs (approximately 0.5° grids) used in this study are too coarse to be effectively applied in hydrological impacts studies and a further downscaling step is therefore required. One of the simplest downscaling methods that has been applied in hydrological impacts assessment is the bias-correction approach (e.g. Fowler and Kilsby, 2007; Kleinn et al., 2005). In this approach, biases in climate model control simulations of the mean monthly climatology for the relevant grid cell relative to station observations are calculated (calculated as a simple difference for temperature and a ratio for precipitation). This bias is assumed to be the same for the future simulations and so corrected climate change scenarios may therefore be obtained by applying the same bias corrections additively to daily temperature and as a scalar to daily precipitation values for future time periods. However, this method only applies the correction to the mean and does not take account of model deficiencies in reproducing observed variability. We therefore adopt the quantile-based mapping approach to bias correction described by Wood et al. (2004) which has been previously used in hydrological impacts studies (e.g. Salathé et al., 2007). This mapping approach uses an empirical transfer function (e.g. Panofsky and Brier, 1968) to force the probability distributions of the control simulations of daily temperature and precipitation to match the observed distributions. Separate mapping functions are calculated on a monthly basis for each station using the appropriate grid cell from each model. Thus, for each RCM, the distributions of daily temperature and precipitation for the control simulation are corrected to match those of the observed data, and are identical for each model. Under the assumption

that model biases are stationary in time, the same transfer functions are therefore applied to adjust the temperature and precipitation scenarios for the 2071-2100 time period.

For many hydrologists and water resource planners, scenarios for the end of the 21st century do not adequately reflect the most appropriate timescales for decision-making and planning. More frequently management decisions are made for the near-future, on decadal rather than century timescales. To address these needs, scenarios were also produced for two additional time periods: 2011-2040 and 2041-2070. To produce these we adopted a conventional pattern scaling approach (Mitchell, 2003; Santer et al., 1990), assuming that changes to mean climate parameters will occur in proportion to the projected change in global mean temperature. This method has been used to construct climate change scenarios for hydrological impact studies (e.g. Salathé, 2005) and has been applied to the scaling of changes in different climatic variables for different geographic regions and time periods (e.g. Mitchell et al., 1999; Santer et al., 1994; Tebaldi et al., 2004). The changes in mean monthly temperature and total monthly precipitation were therefore scaled for the relevant time periods in proportion to the mean global temperature change projected by the GCM which provided lateral boundary conditions for each RCM simulation (either HadCM3 or ECHAM4) using data available from the IPCC data distribution centre[5].

4.3 Projected changes in local climate

The climate change scenarios show a general increase in temperature throughout the year (Figure 8A). The annual mean temperature increase for Bierset ranges from +3.5°C (HIRHAM_H) to +5.6°C (RCAO_E) with the projected change strongly influenced by the GCM used to drive the RCM simulations. Simulations driven by GCM ECHAM4/OPYCA2 (scenarios HIRHAM_E and RCAO_E, see Table 8) project the greatest increases, particularly

23

during spring and summer. Although all models project the largest temperature increases during summer with the maximum increases in August, those by HIRHAM_E (~7.5°C) and RCAO_E (~9.5°C) are larger than those projected by the other models (+4.7°C to +6.4°C). All models project the smallest temperature increases during late winter/early spring ranging from ~+2°C (RCAO_H; March) to ~+5.5°C (RCAO_E; March).

The RCMs consistently project a decrease in annual precipitation but there is a large range from −1.9 % (ARPEGE_H) to −15.3 % (HAD_P_H) (Figure 8B). These precipitation decreases are a consequence of large projected decreases during summer months but are partly offset by increases in winter precipitation. The largest summer decreases are projected by RCAO_E but these are also offset by the largest winter increases projected by any of the models. The large annual decrease projected by HAD_P_H however arises as a consequence of moderate decreases in summer precipitation that persist throughout autumn and are only offset by comparatively small increases during winter.

All models therefore suggest that by the end of the century, the climate of the Geer basin will consist of warmer, wetter winters and much hotter, drier summers, with a more pronounced annual cycle of temperature and precipitation. Given the decreased summer rainfall, higher evapotranspiration driven by higher temperatures and the projected regional increase in the frequency of summer droughts (Blenkinsop and Fowler, 2007), increased stress is likely to be placed on water resources during summer. During winter, higher evapotranspiration could be offset by increased rainfall. The main form of uncertainty lies in the magnitude of the annual groundwater recharge change and how quickly significant impacts on groundwater reserves will be felt.

---

[5] http://www.ipcc-data.org/

4.4 Projected changes in hydrological regime

Using the calibrated flow model and the six downscaled RCM scenarios, hydrological simulations were run to evaluate the direct climate change impacts on the groundwater system of the Geer catchment for the three time periods 2011-2040, 2041-2070 and 2071-2100 using the bias-corrected temperature and precipitation scenarios. As the bias-correction of each climate scenario reflects control simulation biases relative to observations, future changes are expressed relative to an additional hydrological 'control simulation' driven by the observed climate data. Monthly PET are derived from temperature data using the correlation derived between PET calculated with the Thornthwaite formula (Thornthwaite, 1948), and monthly PET measured at the 'Bierset' climatic station. Groundwater abstraction flow rates (from wells and from the draining galleries) are kept constant through all simulations. As for the calibration procedure, initial conditions for each time period and climate change scenario are obtained by running a preliminary steady state simulation with the mean climatic data of the corresponding time period and climate change scenario. Table 9 presents the changes in each of the water balance terms for each time period and each RCM scenario. Figure 9 presents the mean hydraulic head, the standard deviation, minimum and maximum values for each time period, each RCM scenario and each observation well. Similarly, Figure 10 presents the flow statistics at gauging station 'Kanne' for each time period and each RCM scenario. These flow statistics are also presented for summer and winter separately. The significance of differences between the control period and the climate change scenarios was evaluated using statistical t-test[6] with a confidence level of 99% (see Figure 9 and Figure 10).

During 2011-2040, no clear changes from the observed control simulation 1967-1997 can be identified, with large uncertainties projected in the direction of change for both surface

---

[6] Normality of the distributions were checked using Shapiro-Francia normality tests

flow rate and mean groundwater hydraulic head. However, by 2041-2070 and 2071-2100, the simulations project a significant decrease of almost all groundwater levels and flow rate at 'Kanne' compared to the control simulation. By 2071-2100, mean groundwater levels are expected to decrease by 2 m to 8 m depending on location in the Geer basin and the climate change scenario analysed. For an equivalent unsaturated zone depth, which smoothes recharge fluxes, the variability of the groundwater levels is projected to increase. For the same period, flows at Kanne are expected to decrease between 9% and 33%. Figure 10 shows that the decrease in flows is not significant in winter, but in summer all mean flow values and standard deviation intervals for the 2071-2100 time period are lower than the mean flow value of the control period. Generally, the greatest changes are projected by HAD_P_H, which predicts large precipitation decreases during almost the whole year. The smallest changes are projected by ARPEGE_H, which combines a small increase in temperature with a small decrease in precipitation. Table 9 also shows the increasing importance of the evapotranspiration and water abstraction fluxes, compared to the annual rainfall flux which is expected to decrease in the future. However, except for ARPEGE_H, simulations project that actual evapotranspiration rates will decrease, as the general increase in temperature is offset by the decrease in precipitation in summer.

5. Discussion of the results

5.1 Calibration

Climate change simulations indicate that groundwater levels and river flow rates are expected to decrease significantly by 2041-2070 and 2071-2100. Because the calibration of the numerical model is still not perfect, uncertainty remains and may translate into the results of climate change impact studies. In particular, as water balance components are not simulated perfectly (see Section 3.5), this may have an impact on recharge and discharge simulations. Nevertheless, the calibration results show that the model is able to satisfactorily

simulate the multi-annual variations in groundwater levels. Therefore, even though hydraulic heads may be overestimated at some places, the model is able to simulate pluri-annual trends in groundwater levels under long-term climate change scenarios. In addition, the use of an integrated surface – subsurface hydrological models enables a better identification of the errors provided by the model simulations. With a simple subsurface model, high groundwater levels could be explained by low hydraulic conductivities, high recharge rates or low discharge rates. The surface – subsurface model implemented in this study enables us to state that the high groundwater levels are mostly due to errors in the simulation of water balance components. Understanding the causes of model errors gives some reliability to the interpretations and, more generally, gives some credibility to the methodology of using surface – subsurface integrated hydrological models.

5.2 Discretisation

Spatial and temporal discretisations have been chosen to allow the study of long-term variations of groundwater levels and water balance terms under changing climate. Using a discretisation as fine as reported by Jones (2005) and Li et al. (2008) would lead to excessively large simulation times, mostly because of the much longer period covered by the climate change scenarios. However, the objective of the model is not to simulate surface water at the river bed scale, but to provide an accurate representation of the components of water balance at any time during the simulation. Using a model with a coarser discretisation is assumed to be appropriate to study climate change impacts while keeping the computational demand low. The grid used was developed according to this objective.

5.3 Climate change scenarios

As stated in Section 4.1, adopting a multi-model approach for the climate scenarios enables the uncertainty derived from climate model selection to be incorporated into the

assessment of the impacts of climate change on the Geer catchment. The full range of uncertainties in future climate scenarios is not represented in this study, as only six regional climate models from the larger PRUDENCE ensemble have been used. However, the same framework could readily be applied to a larger ensemble size given adequate computational resources. Furthermore, the uncertainty in future emissions is not addressed in this study. Whilst the PRUDENCE project does provide some RCM simulations for the same future time period (2071-2100) for the B2 emissions (medium-low) scenario, the application of these to the groundwater model is unlikely to provide a greater understanding of future uncertainties in the response of the Geer basin. A comparison of the contribution of the various sources of uncertainty within the PRUDENCE model simulations indicates that emission scenario is the most important source only for summer temperatures over southern Europe (Déqué et al., 2007). Generally, the uncertainty introduced by the GCM boundary conditions is larger than that for the other sources whilst the RCM introduces uncertainty of a similar magnitude to that of the GCM boundary conditions only for summer precipitation. Here, the full range of uncertainty generated by the choice of GCM boundary conditions is necessarily constrained by the experimental combinations provided by the PRUDENCE project and has been maximised in terms of the subset of experiments selected in this analysis. However, it is evident that the limited GCM selection applied in PRUDENCE constrains the uncertainty measured from this source (Déqué et al., 2007). It is noted that the A2 and B2 scenarios examined by PRUDENCE only constitute 50% of the spread of greenhouse gas concentrations from all SRES scenarios (Déqué et al., 2007) and that impact studies using a larger range of emission scenarios suggest a greater contribution to total uncertainty generated by emissions relative to RCM choice (e.g. Olesen et al., 2007). Nonetheless, this study provides a major advance in the assessment of the uncertainty of the impact of climate change

on groundwater systems and provides a stepping stone for an impact assessment which undertakes a comprehensive examination of uncertainty from all sources.

6. Perspectives

The application of bias-correction techniques to the downscaling of climate model output also imposes another limitation for hydrological applications. Until transient RCM simulations are available, the timeframe of scenarios is constrained by the time periods made available by RCM "time-slice" simulations. Whilst applying a pattern scaling approach does enable scenarios to be made available for other time periods, the method preserves the temporal structure of the RCM output in all scaled periods rather than producing transient scenarios of change. These issues form part of the remit of the Framework VI AquaTerra project under which a framework to address these issues has recently been tested. This framework has been used to provide transient climate scenarios through to 2085 for the Brévilles catchment in northern France. In this approach, a stochastic rainfall model is used to generate 1300 transient rainfall series based on changes projected for 2071-2100 by 13 PRUDENCE RCMs (Burton et al., 2008). A pattern scaling approach is applied to changes in monthly rainfall statistics for each year in the simulation and these series are used to generate daily temperature series using a stochastic weather generator (Blenkinsop et al., 2008). Producing a large ensemble of daily time series enables to reflect the uncertainty due to natural climate variability in future projections. Using these daily time series in catchment scale impact studies would represent a real innovation and would allow climate change impacts on groundwater reserves to be assessed using a probabilistic approach, which is highly sought after for risk management.

As stated in Section 5, the choice of spatial and temporal discretisations is constrained by the computational demand. The next task for this study will be to compare several spatial

and temporal discretisation options in the context of assessing climate change impact on groundwater reserves. The goal is to evaluate what are the consequences of using finer or coarser discretisations, and to help hydrogeologists and modellers optimize models between performance and computing demand. This optimization is crucial to further apply stochastic climate change scenarios to the hydrological model developed in this study. A 90-year simulation using daily input data takes more than 20 days (3.0 GHz Pentium4 desktop machine equipped with 4Gb RAM) while the same simulation using monthly input data takes only 2 days. This makes a huge difference given than stochastic studies require running hundreds of simulations. Different discretisation could also be needed for more specific purposes. Using shorter time steps for limited time periods may be required to study the influence of intense rainfall events on the hydrologic system. Precipitations occurring as more violent events such as storms are likely to induce a significant change in terms of runoff compared to the same amount of precipitation smoothly distributed over large time intervals. A higher resolution of the horizontal spatial discretisation would also be needed to study local effects or phenomena linked to the fluvial dynamics and the river bed configuration.

This study focuses on the direct impacts of climate change on groundwater reserves but other factors may also affect indirectly, but importantly, the groundwater reserves in the context of climate change. Examples of such factors are the evolution of vegetation, and changes to agricultural practices and land use. Drier summers will also likely cause increases in water demand and exploitation rate of groundwater. Intensification of irrigation practices by groundwater extraction will also induce an additional water volume leaving the system by evapotranspiration. Additionally, problems of contaminant accumulation (e.g. salts, pesticides, fertilisers) could also appear because of the circulation in a closed system. All these possible indirect impacts offer opportunities to further use and develop the model to address contaminant transport problems.

7. Summary and conclusion

A surface – subsurface water flow model of the Geer basin has been developed to assess the possible impacts of climate change on the groundwater resources. This model is physically-based, spatially-distributed and it fully integrates the groundwater and surface water components. The model has been calibrated using observations of hydraulic heads and surface water flow rates for the period 1967-2003. Simulations for three time periods (2011-2040, 2041-2070, 2071-2100) were performed using six climate change scenarios developed using output from Regional Climate Models (RCMs) and downscaled to the station scale using a quantile mapping bias-correction technique. The models consistently project a pattern of much hotter and drier summers and warmer and wetter winters. Results show that when the climate scenarios are applied to the flow model, significant decreases are expected in the groundwater levels by 2041-2070, with even larger decreases by 2071-2100. Similarly, surface water flow rates are expected to decrease during summer, with stronger and longer periods of low water discharge.

This study presents a robust methodology and guidelines that can be used to assess impacts of climate change on groundwater reserves and the large uncertainties surrounding these. The methodology combines the advantages of a fully-integrated surface – subsurface models, spatially distributed evapotranspiration rates and sophisticated multi-model ensemble climate change scenarios. The use and the combination of these three techniques advance the study of climate change impacts on groundwater reserves. The modelling approach integrating surface flow, subsurface flow and evapotranspiration better represents the interdependent aspect of recharge processes between surface and subsurface domains compared to classical or externally coupled models, which is a key element in the context of assessing potential climate change impacts on groundwater. Using integrated models also enables the better identification of the origin of model inaccuracies in the interpretation of the

results of projections. Integrated surface –subsurface models are usually not used in the context of climate change impact evaluation. Additionally, the calibration performed with the Geer basin model is original as it is performed using both observed hydraulic heads and surface water flow rates. Most studies where fully integrated surface – subsurface hydrological models are used do not present any calibration results for observed subsurface hydraulic heads (Jones, 2005; Li et al., 2008; Sudicky et al., 2008). Van Roosmalen et al. (2007) only use one observation per well to calibrate their model. Additionally, they only present global performance criteria values aggregating hydraulic head error from all observation wells. Consequently, it is impossible to evaluate the quality of the calibration regarding spatial and temporal variations. In this study, the climate change scenarios use a multi-model ensemble of RCMs. Doing so, uncertainties in the multi-model response resulting from structural and parameterisation deficiencies within these climate models can be analysed and the uncertainties surrounding the hydrological response better understood. Scenarios developed from RCMs also offer an advance over those developed using GCMs. It has been shown that RCMs project much larger increases in summer temperatures than their parent GCM and they can project very different changes in precipitation patterns due to their resolving of regional-scale processes (Jacob et al., 2007); these have important implications for changes to groundwater processes. Therefore, the downscaling method used in this study provides a state-of-the-art method with which to assess climate change impacts on hydrologic systems.

The results and tools presented above are highly important for river basin management as groundwater storage will be one of the key measures readily exploitable to mitigate potential decreases of water availability due to climate change. The methodology also offers interesting perspectives in terms of indirect impacts of climate change and risk assessment using stochastic climate change scenarios.

Acknowledgements

References

Allen, D.M., Mackie, D.C. and Wei, M., 2004. Groundwater and climate change: a sensitivity analysis for the Grand Forks aquifer, southern British Columbia, Canada. Hydrogeology Journal, 12(3): 270-290.

Arnell, N.W., 2003. Relative effects of multi-decadal climatic variability and changes in the mean and variability of climate due to global warming: future streamflows in Britain. Journal of Hydrology, 270(3-4): 195-213.

Asner, G.P., Scurlock, J.M.O. and Hicke, J.A., 2003. Global synthesis of leaf area index observations: implications for ecological and remote sensing studies. Global Ecology & Biogeography, 12(3): 191-205.

Batlle-Aguilar, J., Orban, P., Dassargues, A. and Brouyère, S., 2007. Identification of groundwater quality trends in a chalk aquifer threatened by intensive agriculture in Belgium. Hydrogeology Journal, 15(8): 1615-1627.

Blenkinsop, S. and Fowler, H.J., 2007. Changes in European drought characteristics projected by the PRUDENCE regional climate models. International Journal of Climatology, 27: 1595-1610.

Blenkinsop, S., Fowler, H.J., Harpham, C., Burton, A., Kilsby, C.G. and Jones, P.D., 2008. Modelling transient climate change. Part 2:Weather Generator and projected changes for the Brévilles catchment. Journal of hydrology, submitted.

Breuer, L., Eckhardt, K. and Frede, H.-G., 2003. Plant parameter values for models in temperate climates. Ecological Modelling, 169: 237-293.

Brouyère, S., 2001. Etude et modélisation du transport et du piégeage des solutés en milieu souterrain variablement saturé (Study and modelling of transport and retardation of solutes in variably saturated media). PhD Thesis, University of Liège, Liège (Belgium), 640 pp.

Brouyère, S., Carabin, G. and Dassargues, A., 2004a. Climate change impacts on groundwater resources: modelled deficits in a chalky aquifer, Geer basin, Belgium. Hydrogeology Journal, 12: 123-134.

Brouyère, S., Dassargues, A. and Hallet, V., 2004b. Migration of contaminants through the unsaturated zone overlying the Hesbaye chalky aquifer in Belgium: a field investigation. Journal of Contaminant Hydrology, 72(1-4): 135-164.

Burton, A., Fowler, H.J., Blenkinsop, S. and Kilsby, C.G., 2008. Modelling transient climate change. Part 1: Developing a transient Neyman-Scott Rectangular Pulses stochastic rainfall model. Journal of hydrology, submitted.

Canadell, J., Jackson, R.B., Ehrlinger, J.R., Mooney, H.A., O.E., S. and Schulze, E.D., 1996. Maximum rooting depth of vegetation types at the global scale. Oecologia, 108: 583-595.

Chen, Z., Grasby, S.E. and Osadetz, K.G., 2002. Predicting average annual groundwater levels from climatic variables: an empirical model. Journal of Hydrology, 260: 102-117.

Christensen, J.H., Carter, T.R., Rummukainen, M. and Amanatidis, G., 2007. Evaluating the performance and utility of regional climate models: The PRUDENCE project. Climatic Change, 81(Supplement 1): 1-6.

Christensen, N.S., Wood, A.W., Voisin, N., Lettenmaier, D.P. and Palmer, R.N., 2004. Effects of climate change on the hydrology and water resources of the Colorado river basin. Climatic Change, 62: 337-363.

Dassargues, A. and Monjoie, A., 1993. The chalk in Belgium. In: R.A. Downing, M. Price and G.P. Jones (Editors), The hydrogeology of the chalk of the North-West Europe. Oxford University Press, Oxford, UK, pp. Chapter 8: 153 - 269.

Déqué, M. et al., 2007. An intercomparison of regional climate simulations for Europe: assessing uncertainties in model projections. Climatic Change, 81(0): 53-70.

Ebel, B.A. and Loague, K., 2006. Physics-based hydrologic-response simulation: Seeing through the fog of equifinality. Hydrological processes, 20(13): 2887-2900.

Fowler, H. and Kilsby, C., 2007. Using regional climate model data to simulate historical and future river flows in northwest England. Climatic Change, 80(3): 337-367.

Fowler, H.J., Blenkinsop, S. and Tebaldi, C., 2007a. Linking climate change modelling to impacts studies: recent advances in downscaling techniques for hydrological modelling. International Journal of Climatology, 27(12): 1547-1578.

Fowler, H.J., Kilsby, C.G. and O'Connell, P.E., 2003. Modelling the impacts of climatic change and variability on the reliability, resilience and vulnerability of a water resource system, Water Resources Research, pp. 10.

Fowler, H.J., Kilsby, C.G. and Stunell, J., 2007b. Modelling the impacts of projected future climate change on water resources in northwest England. Hydrology and Earth System Sciences, 11(3): 1115-1126.

Gordon, C., Cooper, C., Senior, C.A., Banks, H., Gregory, J.M., Johns, T.C., Mitchell, J.F.B. and Wood, R.A., 2000. The simulation of SST, sea ice extents and ocean heat transports in a version of the Hadley Centre coupled model without flux adjustments. Climate Dynamics, 16(2): 147-168.

Hallet, V., 1998. Étude de la contamination de la nappe aquifère de Hesbaye par les nitrates: hydrogéologie, hydrochimie et modélisation mathématique des écoulements et du transport

en milieu saturé (Contamination of the Hesbaye aquifer by nitrates: hydrogeology, hydrochemistry and mathematical modeling). PhD Thesis, University of Liège, Liège (Belgium), 361 pp.

Holman, I., 2006. Climate change impacts on groundwater recharge- uncertainty, shortcomings, and the way forward? Hydrogeology Journal, 14(5): 637-647.

Hornberger, M.G., Raffensperger, J.P., Wilberg, P.L. and Eshleman, K.L., 1998. Elements of Physical Hydrology. JUH Press, 312 pp.

Jacob, D. et al., 2007. An inter-comparison of regional climate models for Europe: model performance in present-day climate. Climatic Change, 81(Supplement 1): 31-52.

Jiang, T., Chen, Y.D., Xu, C.-y., Chen, X., Chen, X. and Singh, V.P., 2007. Comparison of hydrological impacts of climate change simulated by six hydrological models in the Dongjiang Basin, South China. Journal of Hydrology, 336(3-4): 316-333.

Jones, J.-P., 2005. Simulating Hydrologic Systems Using a Physically-based Surface-Subsurface Model: Issues Concerning Flow, Transport and Parameterization. PhD Thesis, University of Waterloo, Waterloo (Canada), 145 pp.

Kleinn, J., Frei, C., Gurts, J., Lüthi, D., Vidale, P.L. and Schär, C., 2005. Hydrologic simulations in the Rhine basin driven by a regional climate model. Journal of Geophysical Research, 110: 18.

Kristensen, K.J. and Jensen, S.E., 1975. A Model For Estimating Actual Evapotranspiration From Potential Evapotranspiration. Nordic Hydrology, 6: 170-188.

Li, Q., Unger, A.J.A., Sudicky, E.A., Kassenaar, D., Wexler, E.J. and Shikaze, S., 2008. Simulating the multi-seasonal response of a large-scale watershed with a 3D physically-based hydrologic model. Journal of Hydrology, 357(3-4): 317-336.

Loáciga, H.A., 2003. Climate Change and Ground Water. Annals of the Association of American Geographers, 93(1): 30-41.

Mitchell, J.F.B., Johns, T.C., Eagles, M., Ingram, W.J. and Davis, R.A., 1999. Towards the Construction of Climate Change Scenarios. Climatic Change, 41(3): 547-581.

Mitchell, T.D., 2003. Pattern Scaling: An Examination of the Accuracy of the Technique for Describing Future Climates. Climatic Change, 60(3): 217-242.

Nakicenovic, N. et al., 2000. Emissions Scenarios. A Special Report of Working Group III of the Intergovernmental Panel on Climate Change, Cambrigde University Press, Cambridge.

Olesen, J. et al., 2007. Uncertainties in projected impacts of climate change on European agriculture and terrestrial ecosystems based on scenarios from regional climate models. Climatic Change, 81(0): 123-143.

Orban, P., Batlle-Aguilar, J., Goderniaux, P., Dassargues, A. and Brouyère, S., 2006. Description of hydrogeological conditions in the Geer sub-catchment and synthesis of available data for groundwater modelling. Deliverable R3.16, AquaTerra (Integrated Project FP6 no 505428).

Panofsky, H.A. and Brier, G.W., 1968. Some applications of statistics to meteorology. The Pennsylvania State University, University Park, 224 pp.

Pope, V.D., Gallani, M.L., Rowntree, P.R. and Stratton, R.A., 2000. The impact of new physical parametrizations in the Hadley Centre climate model: HadAM3. Climate Dynamics, 16(2): 123-146.

Prudhomme, C., Reynard, N. and Crooks, S., 2002. Downscaling of global climate models for flood frequency analysis: where are we now? Hydrological processes, 16(6): 1137-1150.

Rahmstorf, S., Cazenave, A., Church, J.A., Hansen, J.E., Keeling, R.F., Parker, D.E. and Somerville, R.C.J., 2007. Recent Climate Observations Compared to Projections. Science, 316(5825): 709-.

Roeckner, E. et al., 1996. The atmospheric general circulation model ECHAM-4: model description and simulation of present-day climate. Report n° 218, Max-Planck Institute for Meteorology, Hamburg, Germany.

Salathé, E.P., 2005. Downscaling simulations of future global climate with application to hydrologic modelling. International Journal of Climatology, 25(4): 419-436.

Salathé, E.P., Mote, P.W. and Wiley, M.W., 2007. Review of scenario selection and downscaling methods for the assessment of climate change impacts on hydrology in the United States pacific northwest. International Journal of Climatology, 27(12): 1611-1621.

Santer, B.D., Brüggemann, W., Cubasch, U., Hasselmann, K., Höck, H., Maier-Reimer, E. and Mikolajewica, U., 1994. Signal-to-noise analysis of time-dependent greenhouse warming experiments. Climate Dynamics, 9(6): 267-285.

Santer, B.D., Wigley, T.M.L., Schlesinger, M.E. and Mitchell, J.F.B., 1990. Developing climate scenarios from equilibrium GCM results. Rpt. No. 47, Max-Plandk-Institut-fur-Meteorologie, Hamburg (Germany).

Scibek, J. and Allen, D.M., 2006. Modeled impacts of predicted climate change on recharge and groundwater levels. Water Resources Research, 42: 18.

Scibek, J., Allen, D.M., Cannon, A.J. and Whitfield, P.H., 2007. Groundwater-surface water interaction under scenarios of climate change using a high-resolution transient groundwater model. Journal of Hydrology, 333(2-4): 165-181.

Scurlock, J.M.O., Asner, G.P. and Gower, S.T., 2001. Worldwide Historical Estimates of Leaf Area Index, 1932-2000, prepared for the Oak Ridge National Laboratory. ORNL/TM-2001/268, Oak Ridge, Tennessee.

Serrat-Capdevila, A., Valdés, J.B., Pérez, J.G., Baird, K., Mata, L.J. and Maddock Iii, T., 2007. Modeling climate change impacts - and uncertainty - on the hydrology of a riparian system: The San Pedro Basin (Arizona/Sonora). Journal of Hydrology, 347(1-2): 48-66.

Sudicky, E.A., Jones, J.-P., Park, Y.-J., Brookfield, E.A. and Colautti, D., 2008. Simulating complex flow and transport dynamics in an integrated surface-subsurface modeling framework. Geosciences Journal, 12(2): 107-122.

Tebaldi, C., Nychka, D. and Mearns, L.O., 2004. From global mean responses to regional signals of climate change: simple pattern scaling, its limitations (or lack of) and the uncertainty in its results. Proceedings of the 18th Conference of Probability and Statistics in the Atmospheric Sciences, AMS Annual Meeting, Seattle (U.S.A.).

Therrien, R., McLaren, R.G., Sudicky, E.A. and Panday, S.M., 2005. HydroGeoSphere. A three-dimensional numerical model describing fully-integrated subsurface and surface flow and solute transport, 343 pp.

Thornthwaite, C.W., 1948. An approach toward a rational classification of climate. Geographical Rev., 38: 55-94.

Van Roosmalen, L., Christensen, B.S.B. and Sonnenborg, T.O., 2007. Regional Differences in Climate Change Impacts on Groundwater and Stream Discharge in Denmark. Vadose Zone J, 6(3): 554-571.

VanRheenen, N.T., Wood, A.W., Palmer, R.N. and Lettenmaier, D.P., 2004. Potential Implications of PCM Climate Change Scenarios for Sacramento–San Joaquin River Basin Hydrology and Water Resources. Climatic Change, 62(1): 257-281.

Vázquez, R.F. and Feyen, J., 2003. Effect of potential evapotranspiration estimates on effective parameters and performance of the MIKE SHE-code applied to a medium-size catchment. Journal of Hydrology, 270(3-4): 309-327.

Wilby, R.L. and Wigley, T.M.L., 1997. Downscaling general circulation model output: a review of methods and limitations. Progress in Physical Geography, 21(4): 530-548.

Woldeamlak, S., Batelaan, O. and De Smedt, F., 2007. Effects of climate change on the groundwater system in the Grote-Nete catchment, Belgium. Hydrogeology Journal, 15(5): 891-901.

Wood, A.W., Leung, L.R., Sridhar, V. and Lettenmaier, D.P., 2004. Hydrologic Implications of Dynamical and Statistical Approaches to Downscaling Climate Model Outputs. Climatic Change, 62(1): 189-216.

Yusoff, I., Hiscock, K.M. and Conway, D., 2002. Simulation of the impacts of climate change on groundwater resources in eastern England. Geological Society, London, Special Publications, 193(1): 325-344.

Tables

Table 1 : Parameters used in the flow model

	K	Full Saturated hydraulic conductivity	$[L.T^{-1}]$
	n	Total porosity	[-]
Subsurface domain	Ss	Specific storage	$[L^{-1}]$
	α	Van van Genuchten parameter	[-]
	β	Van van Genuchten parameter	$[L^{-1}]$
	S_{wr}	Residual water saturation	[-]
	L_c	Coupling length	[L]
Surface domain	n_x	Manning roughness coefficient	$[L^{-1/3}T]$
	n_y	Manning roughness coefficient	$[L^{-1/3}T]$
	L_e	Evaporation depth	[L]
	θ_{e1} θ_{e2}	Evaporation limiting saturations	[-]
	LAI	Leaf Area Index	[-]
Evapotranpisration	L_r	Root depth	[L]
	C_1, C_2, C_3	Transpiration fitting parameters	[-]
	θ_{t1} θ_{t2}	Transpiration limiting saturations	[-]
	C_{int}	Canopy storage parameter	[L]

Table 2 : van Genuchten parameters, total porosity and specific storage

	Van Genuchten parameters		Residual water saturation	Total porosity	Specific storage
	α [-]	β [l^{-1}]	S_{wr} [-]	n [-]	S_s [L^{-1}]
Chalk formations	0.099	1.10	0.023	0.44	1×10^{-4}
Loess formations	0.076	1.16	0.024	0.41	1×10^{-4}

Table 3 : Hydraulic conductivities values of the calibrated zones (results of calibration)

	name	Saturated hydraulic conductivity [m s^{-1}]
Lower chalk	Chalk 1	4×10^{-5}
	Chalk 2	1×10^{-3}
	Chalk 3	3×10^{-5}
	Chalk 4	2×10^{-6}
	Chalk 5	2×10^{-5}
	Chalk – Dry valleys	2×10^{-4}
Intermediate chalk	Chalk 1	1×10^{-4}
	Chalk 2	1×10^{-3}
	Chalk 3	1×10^{-5}
	Chalk 4	1×10^{-4}
	Chalk 5	5×10^{-5}
	Chalk – Dry valleys	2×10^{-4}
Upper chalk	Chalk 1	1×10^{-4}
	Chalk 2	1×10^{-3}
	Chalk 3	1×10^{-4}
	Chalk 4	1×10^{-4}
	Chalk 5	1×10^{-4}
	Chalk – Dry valleys	2×10^{-4}
	Quaternary loess	1×10^{-8}
	Tertiary deposits	0.3×10^{-7} - 1×10^{-7}

Table 4 : Predefined values for the Manning roughness coefficients and coupling length

	X-Y friction [$L^{-1/3}T$]	Coupling length [$L^{-1/3}T$]
Rural	3	0.01
Urban	0.3	0.01
Forested	6	0.01

Table 5 : Root depths, evaporation depths and Leaf Area Index

	Rural crop (temperate)	Rural grassland (temperate)	Rural broadleaf deciduous forested (temperate)	Urban
Root depth L_r [L]	2.1	2.6	5.2	0.0
Evaporation depth L_e [L]		2.0		
Max. LAI [-]	4.22	2.50	5.12	0.40
C_{int} [L]		1×10^{-5}		
C1 [-]		0.3		
C2 [-]		0.2		
C3 [-]		10		

Table 6 : Mean errors between observed and computed heads for the 9 observation wells
(h^{obs} : observed hydraulic head, h^{comp} : computed hydraulic head, N : number of observations)

	Mean absolute error (L) $$\frac{\sum_i^N \left|\left(h_i^{obs} - h_i^{comp}\right)\right|}{N}$$	Mean error (L) $$\frac{\sum_i^N \left(h_i^{obs} - h_i^{comp}\right)}{N}$$
A7-PL37	7.2	-7.2
BOR009	5.0	3.56
CEL167	4.9	4.9
MOM001	5.5	5.5
OTH002	3.6	2.9
SLI006	8.4	8.4
VIE044	4.5	3.6
WIH014	3.2	0.9
XHE015	1.7	-0.3

Table 7 : mean water balance terms for the period 1967-2003

	Rain	Actual evapotransp.	North boundary	Outlet ('Kanne')	Water abstraction	Water balance error
mm/year	798.6	-502.3	-37.5	-209.2	-51.1	1.5
% of rainfall	100	-62.9	-4.7	-26.2	-6.4	0.2

Table 8 : climate change scenarios with corresponding RCM and GCM
DMI : Danish Meteorological Institute, HC : Hadley Center for Climate Prediction and Research, SMHI : Swedish Meteorological and Hydrological Institute

INST	RCM	GCM	A2 SCENARIO	
			PRUDENCE ACRONYM	AQUATERRA ACRONYM
DMI	HIRHAM	HadAM3H A2	HS1	HIRHAM_H
DMI	HIRHAM	ECHAM4/OPYCA2	ecscA2	HIRHAM_E
HC	HadRM3P	HadAM3P A2	adhfa	HAD_P_H
SMHI	RCAO	HadAM3H A2	HCA2	RCAO_H
SMHI	RCAO	ECHAM4/OPYCA2	MPIA2	RCAO_E
Météo-France	Arpège	HadCM3 A2	DE6	ARPEGE_H

Table 9 : variations of the mean water balance terms for each climate change scenario and time interval

		Rain	Actual evapotransp.	Flux out of North boundary	Flux out of main outlet ('Kanne')	Water abstraction
Control period	mm/year	803.0	-470.6	-39.3	-246.5	-46.6
	% of rainfall	*100*	*-58.6*	*-4.9*	*-30.7*	*-5.8*
HIRHAM H	mm/year	774.6	-456.2	-38.7	-233.1	-46.6
	% of rainfall	*100*	*-58.9*	*-5.0*	*-30.1*	*-6.0*
HIRHAM_E	mm/year	776.9	-463.8	-38.1	-228.4	-46.6
	% of rainfall	100	*-59.7*	*-4.9*	*-29.4*	*-6.0*
HAD_P_H	mm/year	769.6	-442.5	-38.5	-242.0	-46.6
	% of rainfall	*100*	*-57.5*	*-5.0*	*-31.4*	*-6.1*
RCAO_H	mm/year	786.1	-465.4	-38.5	-235.6	-46.6
	% of rainfall	*100*	*-59.2*	*-4.9*	*-30.0*	*-5.9*
RCAO_E	mm/year	786.4	-456.1	-38.5	-245.2	-46.6
	% of rainfall	*100*	*-58.0*	*-4.9*	*-31.2*	*-5.9*
ARPEGE_H	mm/year	799.0	-465.8	-39.2	-247.5	-46.6
	% of rainfall	*100*	*-58.3*	*-4.9*	*-31.0*	*-5.8*
HIRHAM H	mm/year	743.1	-450.3	-37.9	-208.3	-46.6
	% of rainfall	*100*	*-60.6*	*-5.1*	*-28.0*	*-6.3*
HIRHAM_E	mm/year	755.5	-460.9	-37.8	-210.3	-46.6
	% of rainfall	*100*	*-61.0*	*-5.0*	*-27.8*	*-6.2*
HAD_P_H	mm/year	733.0	-442.7	-38.1	-205.6	-46.6
	% of rainfall	*100*	*-60.4*	*-5.2*	*-28.0*	*-6.4*
RCAO_H	mm/year	767.4	-462.7	-38.4	-219.7	-46.6
	% of rainfall	*100*	*-60.3*	*-5.0*	*-28.6*	*-6.1*
RCAO_E	mm/year	772.6	-456.6	-37.9	-231.6	-46.6
	% of rainfall	*100*	*-59.1*	*-4.9*	*-30.0*	*-6.0*
ARPEGE_H	mm/year	794.8	-478.5	-38.9	-230.8	-46.6
	% of rainfall	*100*	*-60.2*	*-4.9*	*-29.0*	*-5.9*
HIRHAM H	mm/year	697.9	-427.8	-37.0	-186.3	-46.6
	% of rainfall	*100*	*-61.3*	*-5.3*	*-26.7*	*-6.7*
HIRHAM_E	mm/year	719.1	-440.1	-36.7	-195.8	-46.6
	% of rainfall	*100*	*-61.2*	*-5.1*	*-27.2*	*-6.5*
HAD_P_H	mm/year	680.6	-431.5	-36.8	-165.8	-46.6
	% of rainfall	*100*	*-63.4*	*-5.4*	*-24.4*	*-6.8*
RCAO_H	mm/year	740.4	-446.5	-37.0	-210.3	-46.6
	% of rainfall	*100*	*-60.3*	*-5.0*	*-28.4*	*-6.3*
RCAO_E	mm/year	750.1	-442.6	-37.5	-223.5	-46.6
	% of rainfall	*100*	*-59.0*	*-5.0*	*-29.8*	*-6.2*
ARPEGE_H	mm/year	788.1	-481.5	-37.8	-222.2	-46.6
	% of rainfall	*100*	*-61.1*	*-4.8*	*-28.2*	*-5.9*

Row groups (left vertical labels): 2011-2040 (HIRHAM H through ARPEGE_H, first block), 2041-2070 (second block), 2071-2100 (third block).

Figures captions

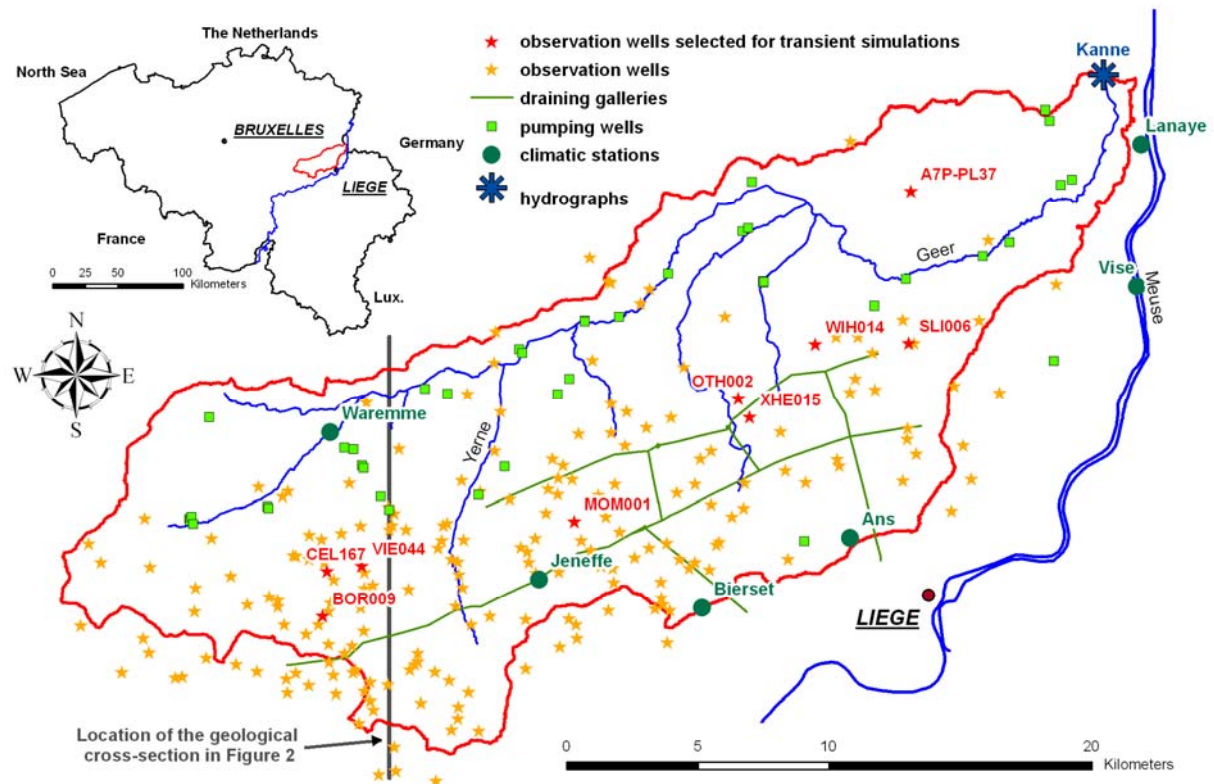Figure 1 : Location of the Geer basin and hydrologic limits

Figure 2 : Geological cross-section in the Hesbaye aquifer (modified from Brouyère *et al*. 2004a), with a vertical exaggeration equal to 40
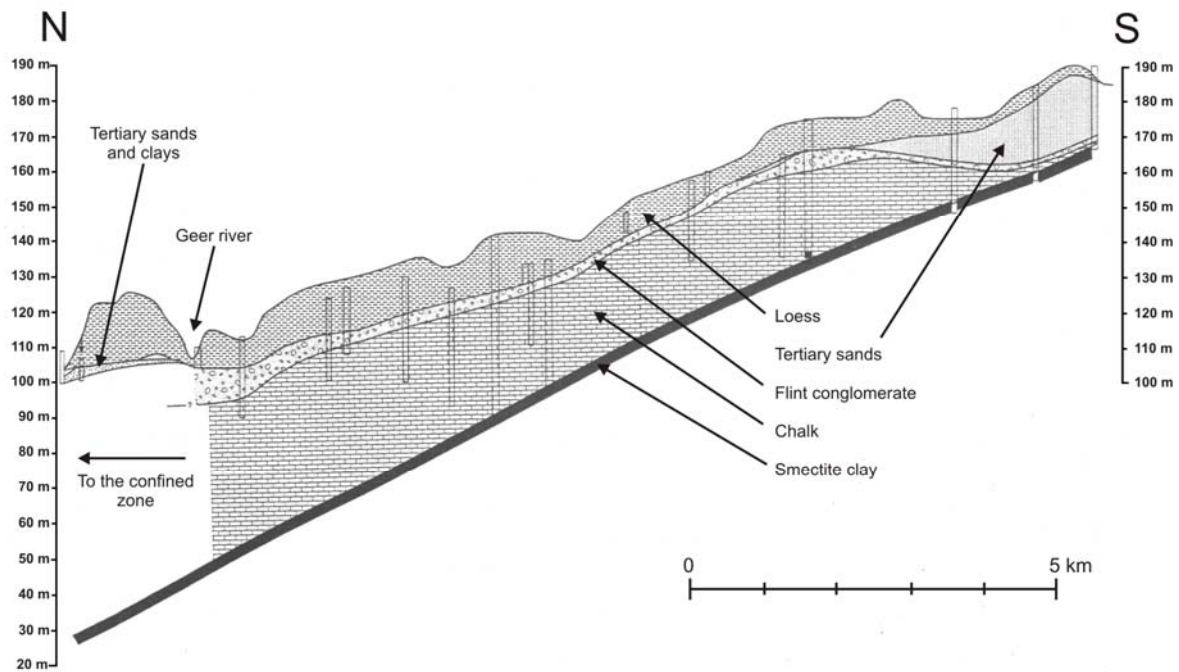
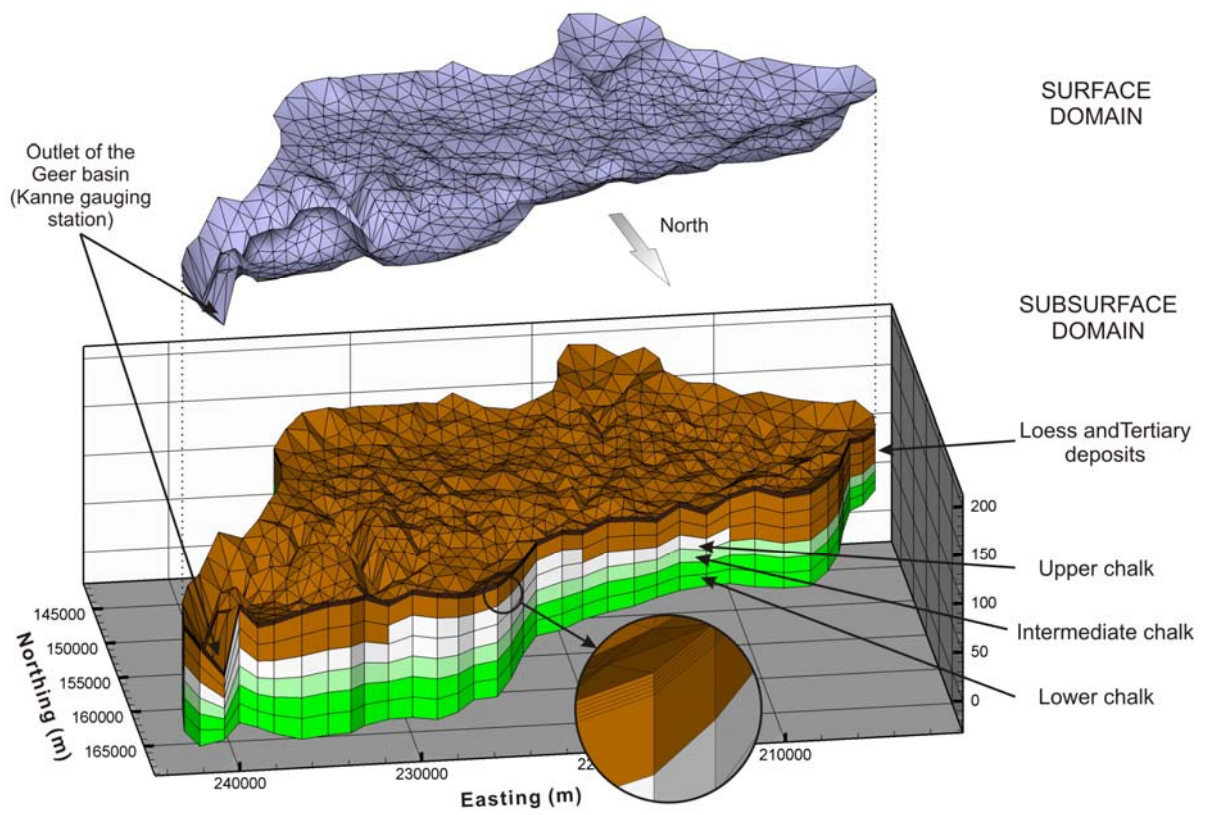Figure 3 : Spatial discretisation of the Geer basin

Figure 4 : Distribution of the hydraulic conductivity zones for the chalk finite elements layers (results of calibration)
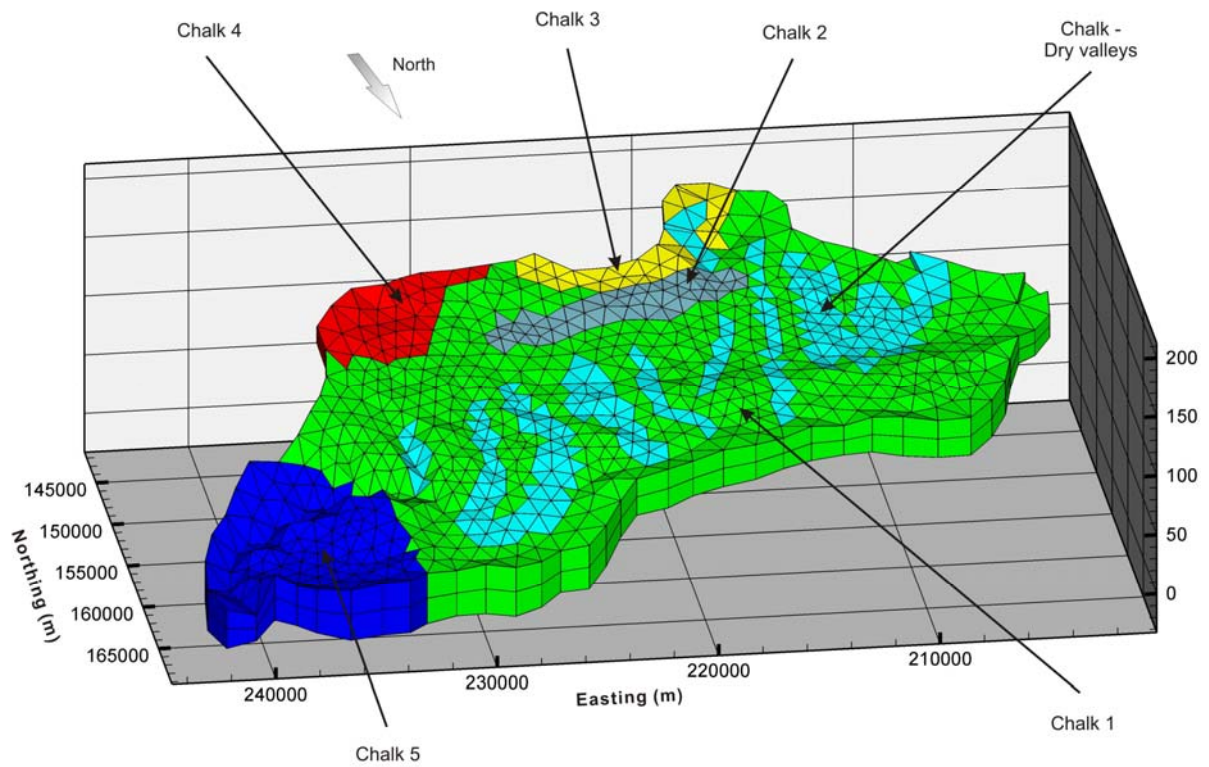
Figure 5 : A. Computed steady-state surface water elevations. B. Computed steady-state subsurface saturation, with full saturation shown in red.
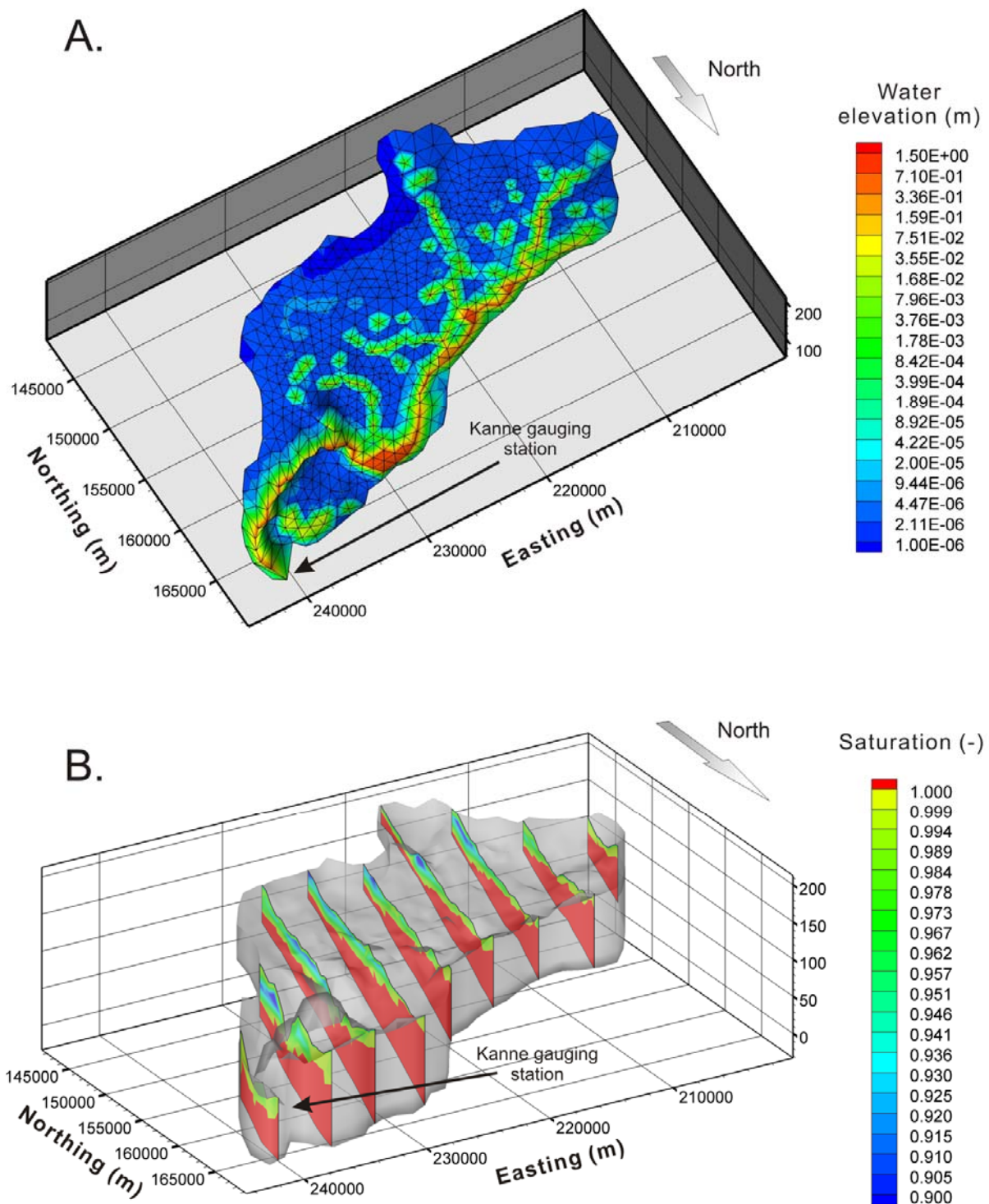
Figure 6 : Transient calibration of hydraulic heads for the 9 observation wells
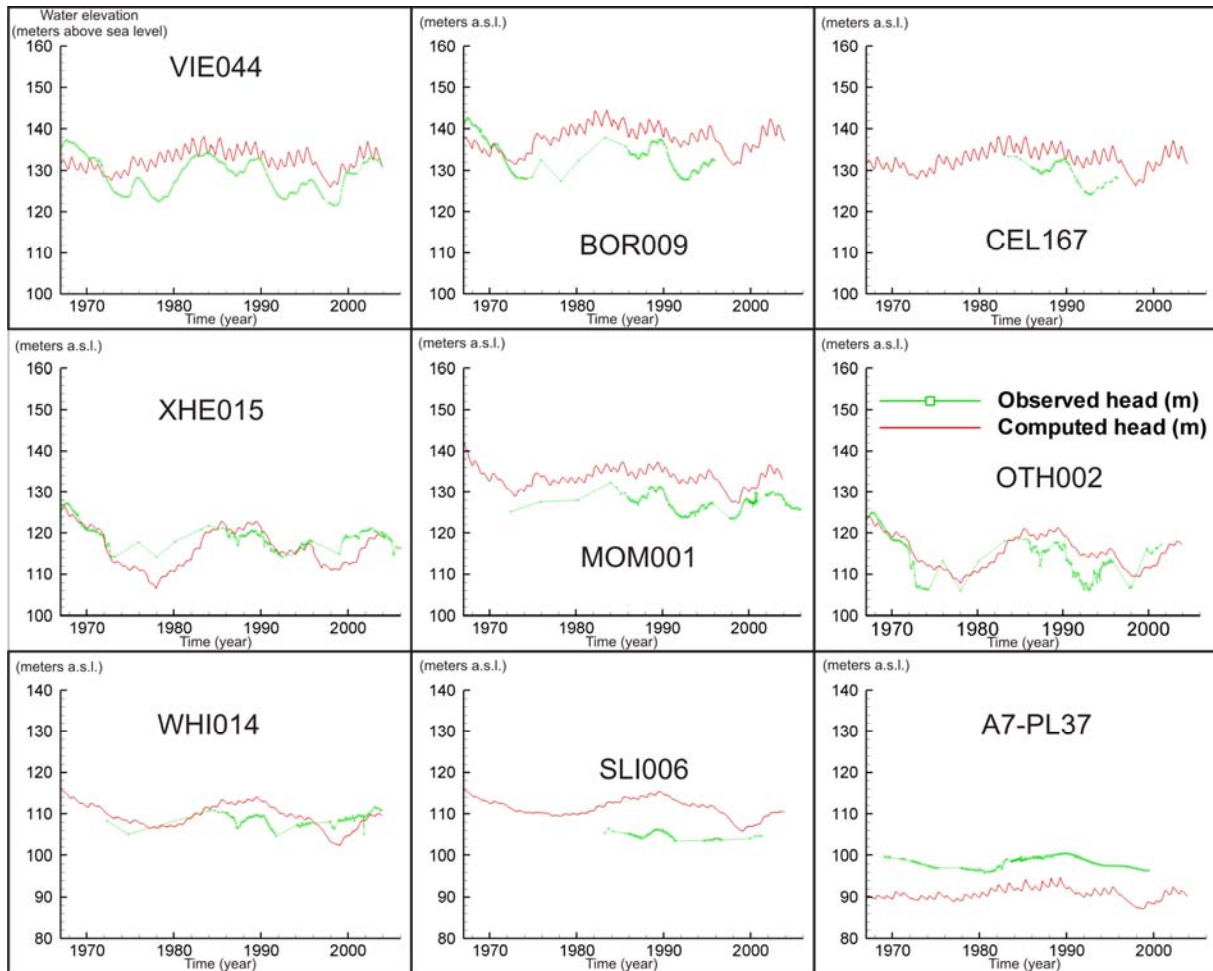
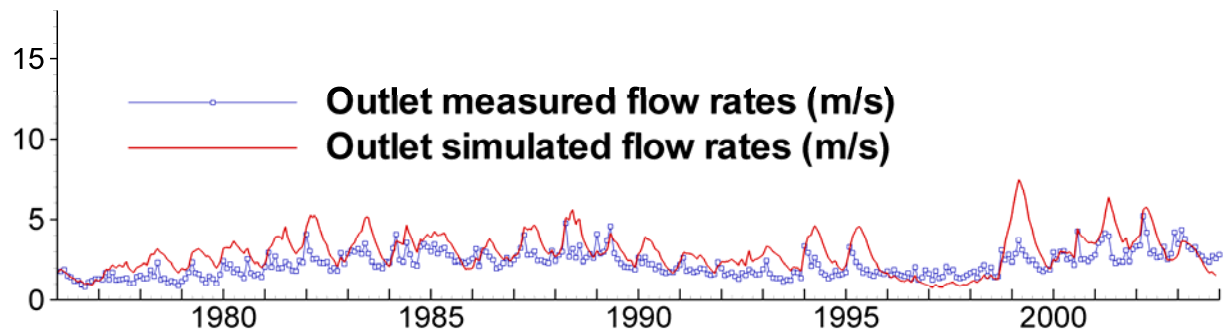Figure 7 : Transient calibration of surface flow rates for the Kanne gauging station (outlet)

Figure 8 : Monthly climatic changes for each climate change scenario (period 2071-2100). A.
Temperature – Bierset climatic station. B. Precipitation – Waremme climatic station.
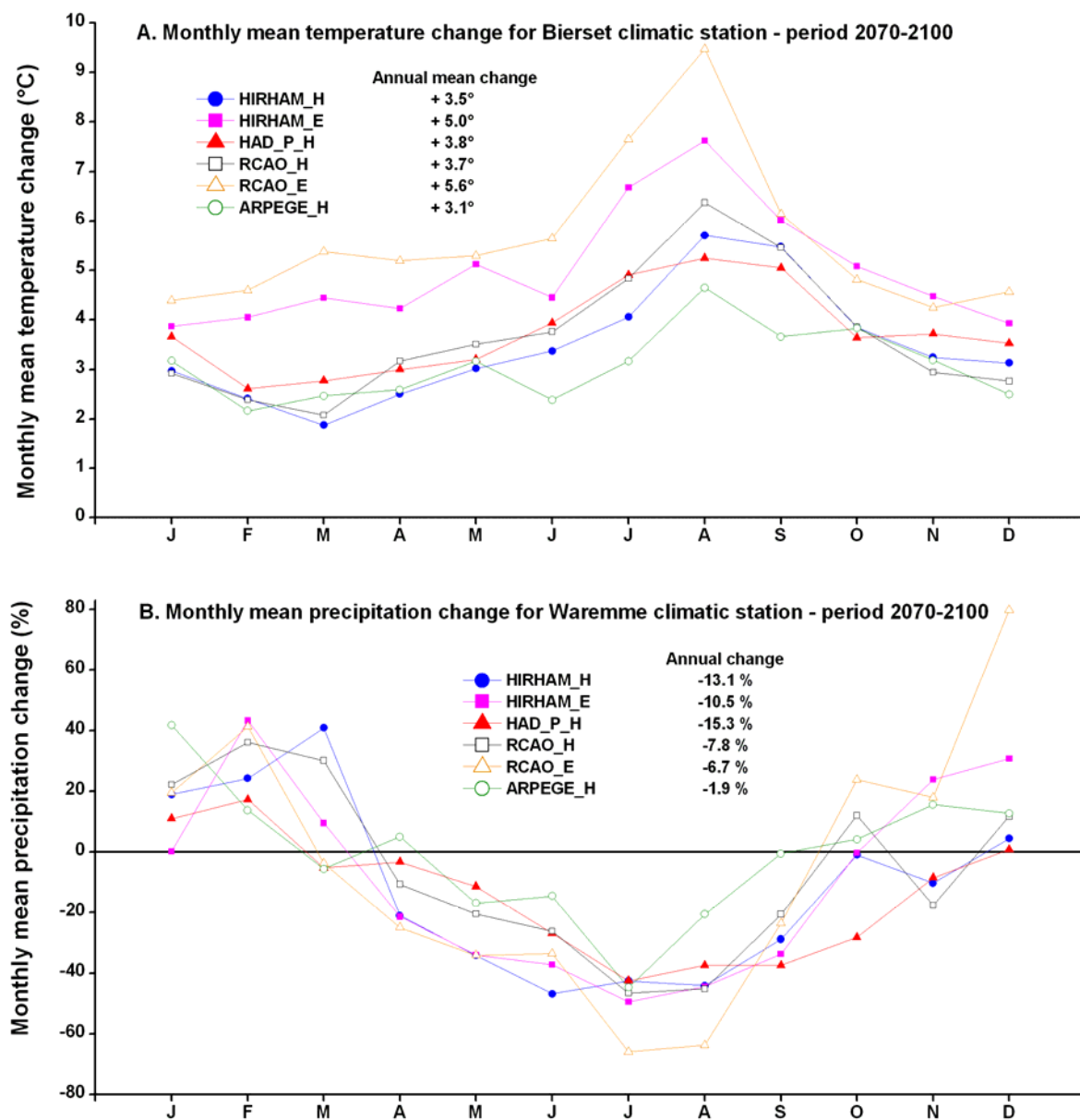
Figure 9 : Evolution of hydraulic heads at the 9 observation wells for each climate change scenario
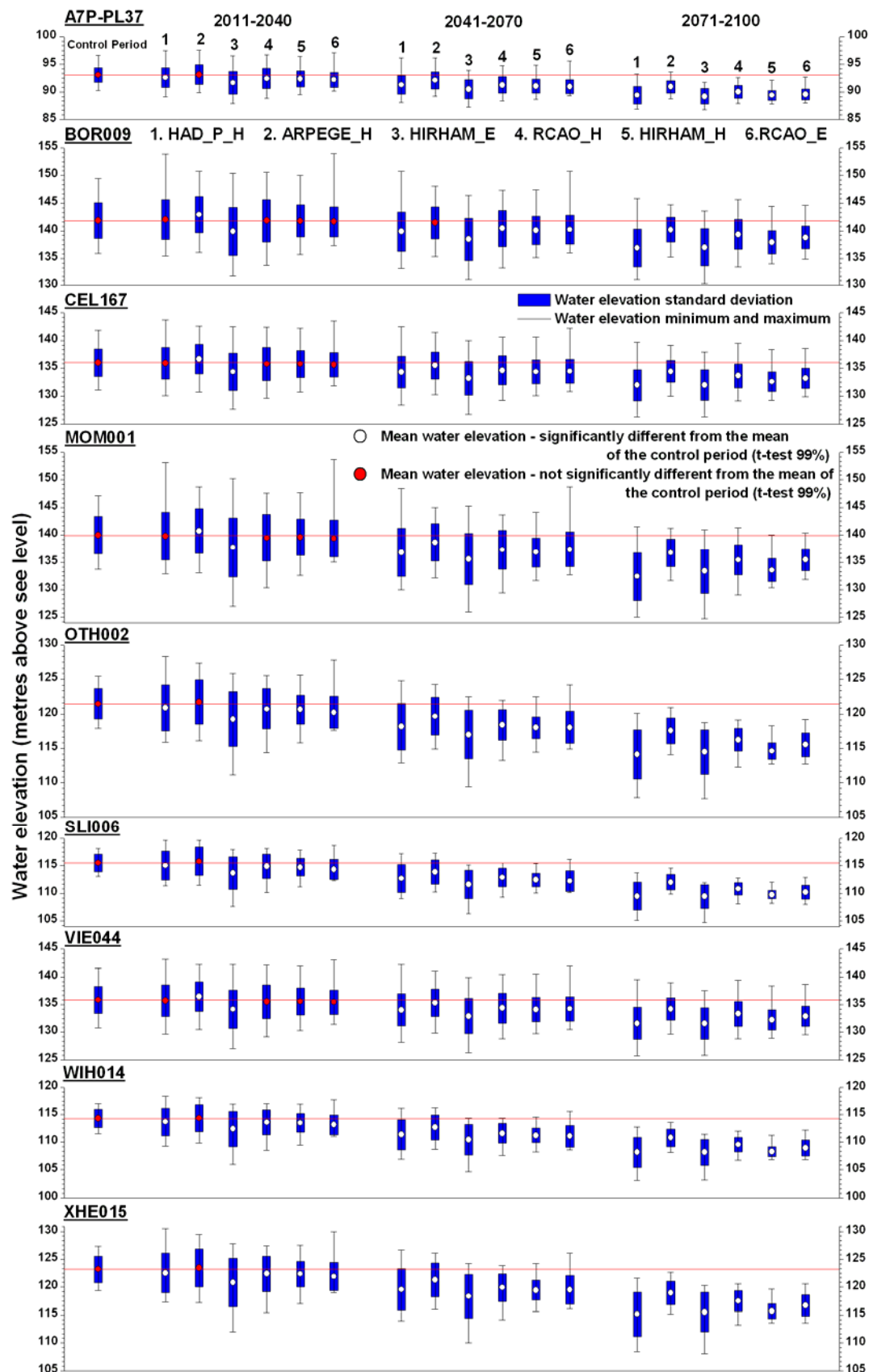
Figure 10 : Evolution of flow rates at gauging station 'Kanne' for each climate change scenario